Carbohydrate Polymers 99 (2014) 728–735

Contents lists available at ScienceDirect

Carbohydrate Polymers

journal homepage: www.elsevier.com/locate/carbpol

Synthesis and properties of novel biomimetic and thermo-responsive dextran-based biohybrids

Fan Li [a,b], Danfeng Pei [b], Qingrong Huang [c], Tongfei Shi [b,**], Guo Zhang [a,*]

[a] Institute of Materials Science and Engineering, Jilin University, Changchun 130023, PR China
[b] State Key Laboratory of Polymer Physics and Chemistry, Changchun Institute of Applied Chemistry, Chinese Academy of Sciences, Changchun 130022, PR China
[c] Food Science Department, Cook College Rutgers University, New Brunswick, NJ 08901-8520, United States

ARTICLE INFO

Article history:
Received 13 June 2013
Received in revised form 22 August 2013
Accepted 4 September 2013
Available online 13 September 2013

Keywords:
Glycopolymer
Dextran
Atom transfer radical polymerization
Polysaccharide
Biodegradable
Nanoparticles

ABSTRACT

A new class of biodegradable, biomimetic and thermo-responsive dextran/synthetic glycopolymer biohybrids (dextran-*graft*-poly(lactobionamidoethyl methacrylate)-*block*-poly(di(ethylene glycol) methyl ether methacrylate), dextran-*g*-(PLAMA-*b*-PDEGMA)), was synthesized by the direct atom transfer radical polymerization (ATRP) of unprotected lactobionamidoethyl methacrylate (LAMA) glycomonomer and di(ethylene glycol) methyl ether methacrylate (DEGMA) monomer. The dextran macroinitiator for ATRP was prepared by partial esterification of the hydroxyl groups of the polysaccharide with 2-bromo-2-methylpropionic acid (BrMPA). The biohybrids containing PDEGMA segments exhibited a lower critical solution temperature (LCST) behavior, which changed from unimers to aggregates in solutions. Moreover, it was demonstrated that these biohybrids had specific biomolecular recognition with ricinus communis agglutinin 120 (RCA_{120}) in comparison with bovine serum albumin (BSA). Furthermore, these biohybrids showed good biocompatibility in the cytotoxicity assays. This hopefully provides a platform for targeted drug delivery and studying the biomolecular recognition between sugar and lectin.

1. Introduction

Glycopolymers, the synthetic polymers containing sugar moieties, have attracted great attention as they can mimic the biological functions of natural oligosaccharides (Voit & Appelhans, 2010). In addition, glycopolymers can present multiple copies of a receptor-binding element that can enhance the binding affinity to receptors, known as the "cluster glycoside effect" (Nagatsuka et al., 2012). As a consequence, glycopolymers are emerging as alternative structures to natural glyco-conjugates (Becer, 2012). The field of glycopolymer synthesis has been expanded dramatically in the past few years by controlled/living polymerization techniques, which enable researchers to design macromolecules of controlled structures (Miura, 2012; Narumi & Kakuchi, 2008; Siegwart, Oh, & Matyjaszewski, 2012). Glycopolymers have been investigated in diverse applications including drug delivery systems (Wang, Zhang, Han, Cheng, & Li, 2012), diagnostic and imaging systems (Pfaff et al., 2011), tissue engineering hydrogels (Polikarpov et al., 2012) and bioactive surfaces (Munoz-Bonilla, Heuts, & Fernandez-Garcia, 2011). However, most of the reported glycopolymers were prepared by the polymerization of vinyl monomers and the resulting polymers were undegradable, despite the fact that degradable polymers are required in most biomedical applications. To address this problem, it is necessary to introduce biodegradable compounds (Dai, Dong, & Yan, 2008; Hu, Fan, & Zhang, 2010; Xu, Wang, Du, & Li, 2009).

Dextran, consisting of mainly $\alpha(1\rightarrow6)$ linked D-glucose units, is the most important commercial available polysaccharides produced by bacterial strains. Owing to its biocompatibility, biodegradability, non-immunogenic and non-antigenic properties, dextran has been widely applied in medicine and pharmacy, such as blood plasma substitute, bio-antifouling materials, etc. (Heinze, Liebert, Heublein, & Hornig, 2006; Sun & Mao, 2012). Moreover, dextran has a low degree of branching, which makes it an optimal starting material for the synthesis of well-defined derivatives. Recently, synthetic polymers such as hydropobic polymers (Lemechko, Renard, Guezennec, Simon-Colin, & Langlois, 2012), stimuli-responsive polymers (Lv et al., 2011) and polyelectrolytes (Wang, Zhu, Chai, Yang, & Xu, 2012) have been grafted onto dextran for their multifunctional properties.

It would be a breakthrough to prepare novel hybrid conjugates of synthetic glycopolymers and natural dextran combining the advantageous properties of both polymers. Using dextran as a backbone could take advantage of its good biodegradability and biocompatibility. Meanwhile, synthetic glycopolymers bearing

* Corresponding author. Tel.: +86 431 85262122.
** Corresponding author. Tel.: +86 135 04705000.
E-mail addresses: tfshi@ciac.ac.cn (T. Shi), fli1216@ciac.ac.cn (G. Zhang).

0144-8617/$ – see front matter © 2013 Elsevier Ltd. All rights reserved.
http://dx.doi.org/10.1016/j.carbpol.2013.09.020

diverse pendent saccharide groups could significantly expand the area of biomedical applications of dextran due to their biorecognition properties. However, to the best of our knowledge, there is no report on preparing biohybrids of synthetic glycopolymers and dextran.

Due to the numerous possible biomedical applications, there is an increasing interest in polymers that exhibit LCST behavior in water. Grafted polymer chains can undergo a transition from hydrophilic to hydrophobic by modifying temperature. So far, a number of dextrans grafting temperature-responsive segments have been reported (Feng et al., 2012; Otsuka et al., 2012; Patrizi, Piantanida, Coluzza, & Masci, 2009) with potential applications as surfactants, drug nanocarriers and controlled released systems. Among the thermosensitive polymers, poly(olig(ethylene glycol)methacrylates) (POEGMA), which is an uncharged, water-soluble, nontoxic polymer, is being developed as new thermoresponsive water-soluble polymer (Lutz, 2011).

Herein, we report the synthesis of dextran biohybrids grafted with synthetic glycopolymers and thermo-responsive segments by ATRP. As an exemplary case, unprotected lactobionamidoethyl methacrylate (LAMA) was chosen as glycomonomer. In addition, the poly(di(ethylene glycol) methyl ether methacrylate) (PDEGMA) segments were grafted on the biohybrids to introduce the thermo responsibility. Here, we employ "grafting from" method, in which the controlled radical polymerization (CRP) techniques are used, rather than "grafting to" method for we can obtain good control over the number, molecular weight and polydispersity of the grafted chains without homopolymer formation and significant degradation of polysaccharide (Bajgai et al., 2009; Dupayage, Save, Dellacherie, Nouvel, & Six, 2008; Wang et al., 2011).

The synthetic strategy was shown in Scheme 1. Firstly, the ATRP initiator molecules were introduced into dextran by esterification reaction. Then, PLAMA segments were grafted onto the dextran by homogeneous ATRP under mild conditions. Last, the PLAMA side chains were proposed to be functionalized by PDEGMA end blocks. The molecular structures, self-assembly, recognition properties and cytotoxicity of as-synthesized dextran-based biohybrids have been characterized by means of Fourier-transform infrared (FT-IR) spectroscopy, ^{1}H NMR, ^{13}C NMR, gel permeation chromatography (GPC), UV–vis spectroscopy, dynamic light scattering (DLS) and cell counting kit-8 (CCK-8) assays.

2. Materials and methods

2.1. Materials

Lactobionamidoethyl methacrylate (LAMA) was synthesized according to the literature (Narain & Armes, 2003). Dextran from *Leuconostoc* spp. ($M_n \sim 23{,}000$ g/mol, $M_w \sim 40{,}300$ g/mol, GPC), 2-bromo-2-methylpropionic acid (BrMPA, 98%), 1,1′-carbonyldiimidazole (CDI, 99%), 4-(dimethylamino)pyridine (DMAP, 99%), anisole (anhydrous 99.7%), dimethyl sulfoxide (DMSO, anhydrous 99.9%), copper(I) chloride (CuCl, 99%), copper(I) bromide (CuBr, 99.999%), di(ethylene glycol) methyl ether methacrylate (DEGMA, 95%) and cell counting kit-8 (CCK-8) were obtained from Sigma–Aldrich Chemical Co. DEGMA was distilled under reduced pressure. 2,2′-Bipyridyl (bpy, 97%), hydroquinone (99%), diethyl ether, methylene dichloride, 2-propanol, triethylamine and methanol were purchased from Sinopharm Chemical Reagent Co. Triethylamine and methanol were vacuum distilled from CaH_2 before use. HepG2 cell line was purchased from the American Type Culture Collection (ATCC, Rockville, MD).

2.2. Synthesis of dextran-macroinitiators (dextran-BrMP$_{8.3}$)

To obtain a derivative with a degree of substitution (DS, the number of 2-bromo-2-methylpropionyl groups introduced for 100 glucose units of dextran) of 8.3%, 2.0 g of dextran (12.3 mmol of glucose residues) and 0.072 g of DMAP (0.6 mmol) were dissolved in 10 mL of anhydrous DMSO at room temperature. In a separate flask, 1 g of BrMPA (6 mmol) and 0.9 g of CDI (5.6 mmol) were dissolved in 10 mL of anhydrous DMSO. The reaction between BrMPA and CDI was carried out at room temperature for 6 h to produce the acylimidazole. After the reaction was complete, the acylimidazole reaction mixture was introduced into the dextran-DMAP solution. The reaction was stirred at 40 °C to produce the dextran-BrMP$_{8.3}$ macroinitiator. The reaction was stopped when the desired DS, as evaluated from the ^{1}H NMR spectrum, was obtained. The final reaction mixture was precipitated with 200 mL of diethyl ether. The crude polymer was purified by precipitation twice in 200 mL of methanol. Finally, the dextran-BrMP$_{8.3}$ was dialyzed (MWCO 6 kDa, 36 h) against distilled water and lyophilized. The actual DS was calculated from the ^{1}H NMR spectrum as described in Section 3.

2.3. Grafting of dextran-macroinitiators with poly(lactobionamidoethyl methacrylate) (dextran-g-PLAMA)

The dextran-*g*-PLAMA polymers were synthesized by the following method. First, dextran-BrMP$_{8.3}$ was dissolved in anhydrous DMSO. Then, predetermined amounts of bpy and LAMA were introduced into the Schlenk reactor. The mixture was thoroughly degassed by three freeze–pump–thaw cycles, and then an appropriate volume of the anisole was transferred in the reactor with a cannula. Afterward, the CuCl (or CuBr) was added to the mixture and was stirred at preset temperature. At this time, the polymerization was started. Typical experimental condition was as follows: $[LAMA]_0 = 0.5$ M, $[anisole]_0 = 0.025$ M, $[LAMA]_0:[Br]_0:[CuCl]_0:[CuCl_2]_0:[bpy]_0 = 40:1:1:0.1:2.5$ (molar ratio), where $[Br]_0$ is the initial concentration of bromide initiating groups, in 10 mL anhydrous DMSO at 20 °C. To follow the conversion yield and the molecular weight, the samples were taken at different intervals. The samples were analyzed by ^{1}H NMR in DMSO-d_6 to evaluate the conversion yield using Eq. (1) from the area of the singlets of LAMA methylene protons (A_{LAMA}, 2H at 5.6 and 6.1 ppm) and that of anisole protons ($A_{anisole}$, 3H at 6.9 ppm)

$$\text{Conversion yield}\,(\%) = 100 \times [1 - (3A_{\text{LAMA,2H}} \times [\text{anisole}]_0)/(2A_{\text{anisole,3H}} \times [\text{LAMA}]_0)] \quad (1)$$

Catalyst residues were removed by passing through a short neutral alumina column. Crude dextran-*g*-PLAMA was precipitated thrice with hot methanol, extensive dialysis against distilled water (MWCO 6 kDa, 48 h) and lyophilized.

2.4. ATRP of DEGMA with dextran-g-PLAMA as macroinitiator

The dextran-*g*-PLAMA can be used as the macroinitiator for the subsequent ATRP of DEGMA to produce the dextran-*g*-(PLAMA-*b*-PDEGMA) comb-like copolymer. The dextran-*g*-(PLAMA-*b*-PDEGMA) was synthesized using a molar feed ratio $[DEGMA]_0:[Cl]_0:[CuCl]_0:[CuCl_2]_0:[bpy]_0 = 79:1:1:0.1:2.5$, where $[Cl]_0$ is the initial concentration of chloride initiating groups, in 10 mL anhydrous DMSO at 45 °C. The ATRP reaction and product purification were performed using the same procedures as those described above.

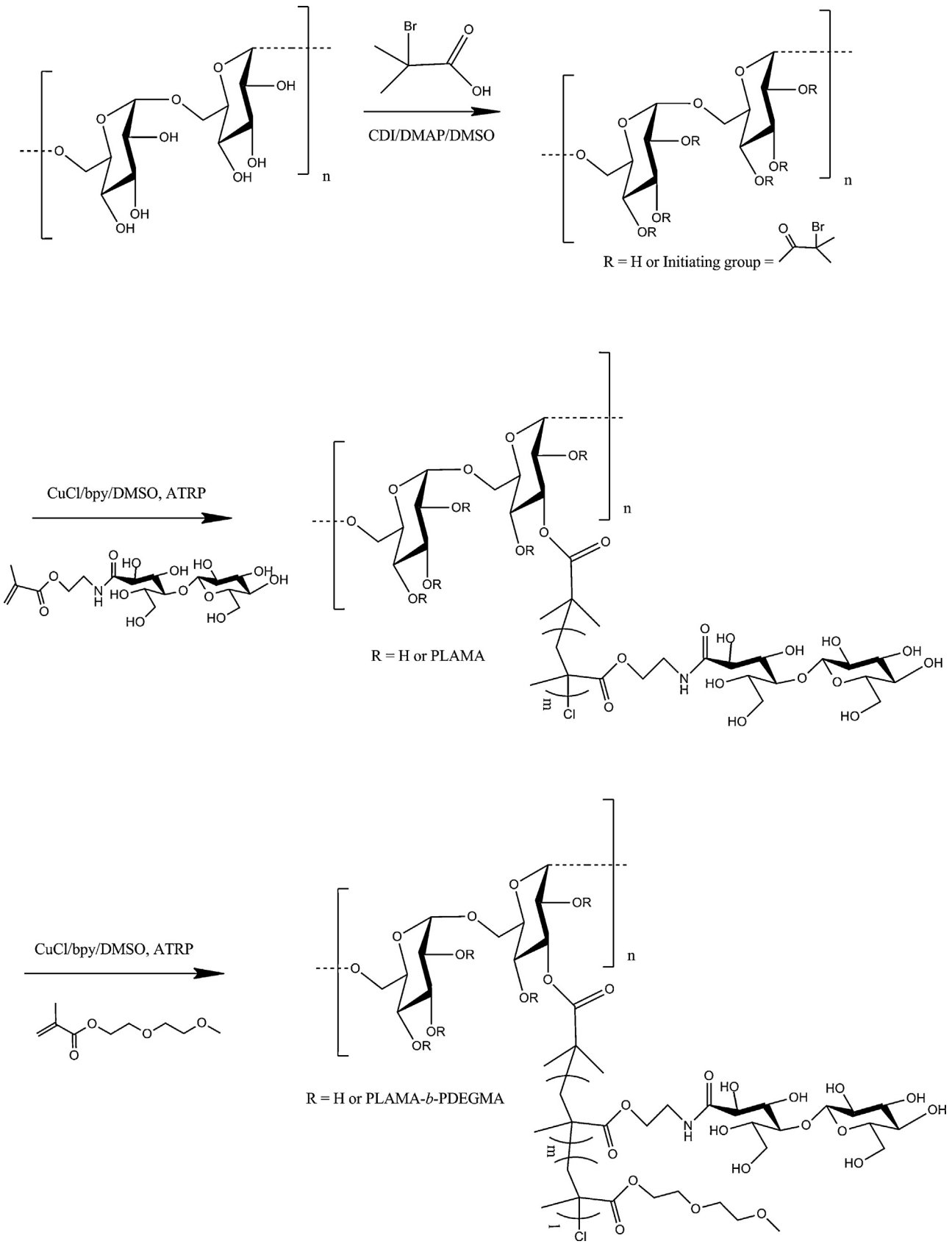

Scheme 1. Synthesis of dextran grafted with PLAMA-*b*-PDEGMA by ATRP.

2.5. Lectin recognition

Agglutinin RCA_{120} and bovine serum albumin (BSA) were purchased from Sigma–Aldrich Chemical Co. A series of the dextran-*g*-PLAMA and dextran-*g*-(PLAMA-*b*-PDEGMA) solutions were prepared by directly dispersing the solid sample in phosphate buffer (pH = 7.4) at different concentrations and stirred 2 h. The lectin recognition activity of the dextran-based conjugates were analyzed by changes in the turbidity of solutions with time at 420 nm following the addition of dextran-based conjugates phosphate buffer solutions into lectin phosphate buffer solutions. Similarly, BSA was used for the control experiments. All the experiments were conducted at 20 °C, lower than the LCST of dextran-*g*-(PLAMA-*b*-PDEGMA) to prevent the thermo-induced self-aggregation.

2.6. Cytotoxicity of the dextran-based biohybrids

Cytotoxicity of the dextran-based biohybrids was evaluated using the CCK-8 assay in HepG2 cell line. The cells were cultured in Dulbecco's modified eagle medium (DMEM), supplemented with 10% fetal bovine serum (FBS), under 5% CO_2 and 95% relative humidity atmosphere. The HepG2 cells were seeded in a 96-well plate at a density of about 10,000 cells/well in 100 μL of growth medium and incubated for 24 h, after which time the growth medium was replaced with DMEM medium containing different concentrations of the dextran-based biohybrids. The preparation of the dextran-based biohybrids stock solutions was as follows. All the dextran-based biohybrids solutions were dissolved into Dulbecco's phosphate buffer at a final concentration of 10 mg/mL. The samples were sterilized by filtered with 0.22 μm syringe filters, and different volumes of prepared solution were added into the DMEM medium. The cells were further incubated for 24 h under the same conditions, after which 10 μL of CCK-8 solution was added to each well, and the plate was incubated for 2 h. Absorbance was measured at 450 nm (PERLONG DNM-9602 plate reader). The cell viability (%) relative to control cells cultured in media without dextran-based biohybrids was calculated from $([A]_{test}/[A]_{control}) \times 100\%$, where $[A]_{test}$ and $[A]_{control}$ are the absorbance values of the wells (with the dextran-based biohybrids) and control wells (without the dextran-based biohybrids), respectively. For each sample, the final absorbance was the average of those measured from four wells in parallel.

2.7. Characterization

^1H NMR and ^{13}C NMR spectra were recorded at room temperature on a Varian Mercury-400 spectrometer. DMSO-d_6 and D_2O were used as the deuterated solvents for the polymers. Molecular weights and molecular weight distributions were assessed by GPC. Chromatograms were recorded using a Varian PL-GPC50plus instrument equipped with a refractive index detector, a Polymer Laboratories guard column (50 mm × 7.5 mm, 10 μm) and two PLgel-Mixed-D (300 × 7.5 mm, 10 μm) columns. The eluent was DMSO with 0.1 M LiBr at a flow rate of 0.6 mL/min at 50 °C. Near-monodisperse dextran standards were used for calibration. Fourier transform infrared (FT-IR) spectra were obtained with a BRUKER VERTEX70 spectrometer at frequencies ranging from 400 to 4000 cm^{-1}. Samples were thoroughly mixed with KBr and pressed into pellet form. UV–vis spectra were recorded at room temperature using a Purkinje General TU-1900 UV–vis spectrophotometer. The mean size of aggregates was determined by dynamic light scattering (DLS) using a Nanotrac wave instrument (MicroTrac, US). The samples were prepared to predetermined concentrations. All the measurements were repeated three times, and the data treatment was done with the Microtrac FLEX software from MictroTrac Inc.

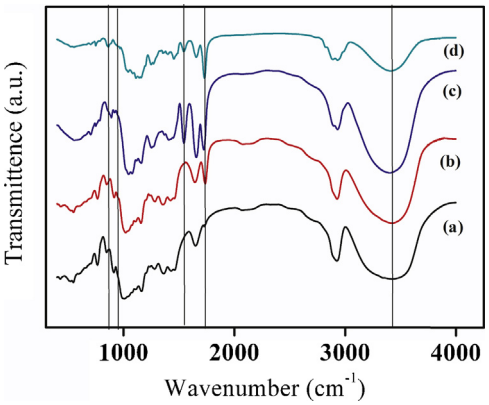

Fig. 1. FT-IR spectra of (a) underivative dextran, (b) Dex-$BrMP_{8.3}$, (c) dextran-*g*-$PLAMA_{23}$ and (d) dextran-*g*-($PLAMA_{23}$-*b*-$PDEGMA_{30}$).

3. Results and discussion

3.1. Synthesis of dextran-macroinitiator (dextran-$BrMP_{8.3}$)

The dextran-macroinitiator (dextran-$BrMP_{8.3}$) was obtained by partial esterification of the hydroxyl groups of the polysaccharide with 2-bromo-2-methylpropionic acid (BrMPA). N,N′-carbonyldiimidazole (CDI) was chosen as esterification reagent in our present work. Because CDI and its by-products are non-toxic, the imidazole and CO_2 formed during the reaction can be easily removed from the polymer, no oxidation or decomposition of the DMSO is observed, and side reaction (e.g. moffatt reaction) can be avoided during the esterification (Heinze et al., 2006). The conversion is followed as a two-stage process. CDI is first reacted with the acid BrMPA to yield the acylimidazole within 6 h at room temperature. Thereby, the tendency of cross-linking initiated by unreacted CDI is avoided. Sequencely, the dextran with a catalyst amount of 4-(dimethylamino)pyridine (DMAP) was added to the acylimidazole to form the required ester. Fig. 1 shows the FT-IR spectrum for the underivatized dextran (curve a, Fig. 1) and dextran-$BrMP_{8.3}$ (curve b, Fig. 1). The stretching vibration of carbonyl in 2-bromo-2-methylpropionyl groups appeared at 1740 cm^{-1} in the FT-IR spectrum of dextran-$BrMP_{8.3}$, but not in that of its precursor, which indicates that the 2-bromo-2-methylpropionyl groups were successfully introduced onto dextran chains. The acylation was further confirmed by ^1H NMR (curve a, Fig. S1) spectrum. In case of DMSO-d_6, the chemical shift in the range of $\delta = 1.9$ ppm and $\delta = 4.7$ could be attributed to the methyl protons of 2-bromo-2-methylpropionyl groups and the anomeric protons of the glucose units, respectively. The degree of substitution (DS, the number of 2-bromo-2-methylpropionyl groups introduced for 100 glucose units of dextran) was estimated using Eq. (2) where $A_{BrMP,6H}$ and $A_{anomeric,H}$ are the integral areas of 2-bromo-2-methylpropionyl protons and anomeric protons of the glucose units, respectively

$$DS = (100/6) \times A_{BrMP,6H}/A_{anomeric,H} \quad (2)$$

The degree of substitution (DS = 8.3%) indicates that every 12 glucose unit of dextran-$BrMP_{8.3}$ possess one initiation site. In this work, the prepared Dex-$BrMP_{8.3}$ with such moderate initiation sites can avoid potential gelation during ATRP due to the radical–radical coupling of the propagating chains from a multifunctional backbone with a high local concentration of initiation sites (Wang, Zhu, et al., 2012). In addition, the concentration of initiation sites can be controlled by adjusting the BrMPA/dextran ratio and reaction time. In the ^{13}C NMR (curve a, Fig.S2) spectrum, the chemical shift of methyl carbon appeared in the range of

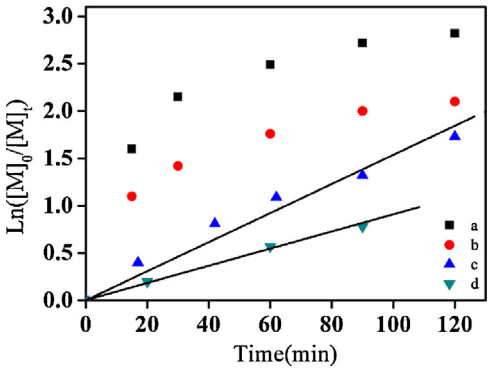

Fig. 2. The $\ln([M]_0/[M]_t)$ versus the reaction time. (a) Dextran-*g*-PLAMA $[LAMA]_0$:$[Br]_0$:$[CuBr]_0$:$[bpy]_0$ = 40:1:1:2, 30 °C, (b) dextran-*g*-PLAMA $[LAMA]_0$:$[Br]_0$:$[CuCl]_0$:$[bpy]_0$ = 40:1:1:2, 30 °C, (c) dextran-*g*-PLAMA $[LAMA]_0$:$[Br]_0$:$[CuCl]_0$:$[CuCl_2]_0$:$[bpy]_0$ = 40:1:1:0.1:2.5, 20 °C and (d) dextran-*g*-(PLAMA-*b*-PDEGMA) $[DEGMA]_0$:$[Cl]_0$:$[CuCl]_0$:$[CuCl_2]_0$:$[bpy]_0$ = 79:1:1:0.1:2.5, 45 °C.

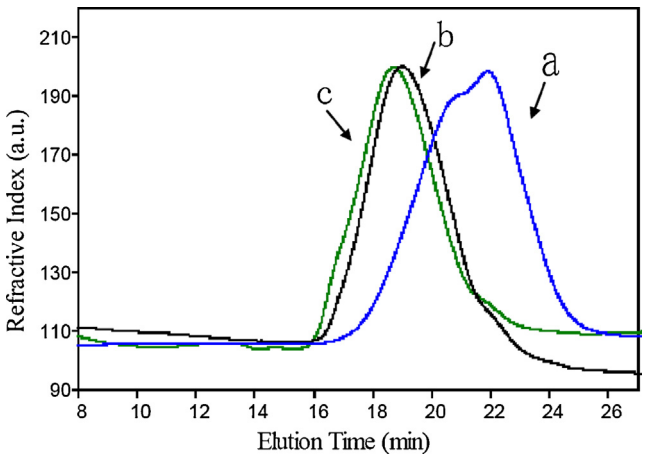

Fig. 3. GPC traces of the biohybrids. (a) Dextran-$BrMP_{8.3}$, (b) dextran-*g*-$PLAMA_{23}$ and (c) dextran-*g*-($PLAMA_{23}$-*b*-$PDEGMA_{30}$).

28 ppm, which is in agreement with 2-bromo-2-methylpropionyl groups graft on dextran backbone.

3.2. Grafting of dextran-macroinitiators with PLAMA

DMSO is an unusual solvent for ATRP. From the literature data, it is known that DMSO could change the nature of the copper catalyst (Monge, Darcos, & Haddleton, 2004). However, the highly water-soluble macroinitiator dextran-$BrMP_{8.3}$ and the monomer LAMA have a very limited solubility in common ATRP solvents. In this work, to obtain homogeneous reaction solutions, polymerizations were performed in DMSO, which is important for ensuring the uniform distribution of grafting polymer chains in the dextran-*g*-PLAMA copolymers.

A preliminary study was done to find the appropriate conditions to control the ATRP of LAMA in DMSO. The ^{1}H NMR spectroscopy was used to estimate the conversion of the PLAMA during the ATRP (Dupayage, Nouvel, & Six, 2011). First assays were conducted at 30 °C with dextran-$BrMP_{8.3}$ as initiator and CuBr/bpy as catalyst: the initial molar ratio of $[LAMA]_0$:$[Br]_0$:$[CuBr]_0$:$[bpy]_0$ was 40:1:1:2 with $[LAMA]_0$ equal to 0.5 mol/L ($[Br]_0$ is the initial concentration of bromide). Anisole was added as internal standard ($[Anisole]_0$ = 0.025 M). As shown in Fig. 2, the observed kinetics was very fast, and more than 67% of the LAMA was polymerized in only 20 min (scatter a, Fig. 2). The rapid polymerization should be related to both the polarity of DMSO and a change in the nature of Cu(I) catalyst by competitive coordination of oxygen atoms of DMSO (Dupayage, Nouvel, & Six, 2012). To improve the control of ATRP, we adopted the mixed halogen initiating system R-Br/CuCl (Matyjaszewski, Shipp, Wang, Grimaud, & Patten, 1998). The reaction was then carried out using $[LAMA]_0$:$[Br]_0$:$[CuCl]_0$:$[bpy]_0$ = 40:1:1:2 in DMSO at 30 °C. Unfortunately, the kinetics plot (scatter b, Fig. 2) showed significant downward curvature after 20 min indicating that reaction of termination occurred. Further, to reduce the polymerization rate and the radical concentration, we decreased the reaction temperature. A little amount of $CuCl_2$ was also added to the polymerization system to prevent irreversible termination reactions which usually occur at the beginning of the polymerization without Cu(II)X (Dupayage et al., 2012). The assays were carried out in DMSO at 20 °C, $[LAMA]_0$:$[Br]_0$:$[CuCl]_0$:$[CuCl_2]_0$:$[bpy]_0$ = 40:1:1:0.1:2.5, [LAMA] = 0.5 M. The kinetic semilogarithmic plot (line c, Fig. 2) showed a reasonable linear dependence of $\ln([M]_0/[M])$ with time up to about 90% conversion (120 min), indicating a constant concentration of propagating species and therefore negligible termination. This phenomenon accorded with the characteristic of ATRP.

FT-IR spectrum of dextran-*g*-PLAMA exhibited a broad overlapped band at 3390 cm^{-1}(curve c, Fig. 1) due to OH and NH stretching. A band at 2900 cm^{-1} was attributed to CH and CH_2 stretching vibrations. The absorbance at 1740 cm^{-1} was due to the carbonyl group. Further, there was a distinct absorbance at 1550 cm^{-1} for the characteristic amide II band within the PLAMA block, which is in agreement with PLAMA grafts on dextran backbone. The ^{13}C NMR spectra in D_2O of dextran-*g*-PLAMA also confirmed the grafting of PLAMA on dextran (Fig. S2), the presence of the signals b, c, d and f is ascribable to the PLAMA chains.

The ^{1}H NMR spectra of dextran-*g*-PLAMA is shown in Fig. S1. The peak at δ = 7.9 was mainly attributable to the amido protons of the PLAMA side chains. In this range of shifts (3.9–5.2 ppm), the peaks corresponded to the anomeric protons and the free OH of PLAMA and dextran. The composition of the grafted copolymers can be confirmed by the integrals of the signals of PLAMA and dextran, based on Eq. (3). $A_{anomeric,dextran}$ and $A_{anomeric,PLAMA}$ are the areas of anomeric protons of dextran and PLAMA, which have chemical shift values of 4.7 and 5.2, respectively

$$DP_{LAMA} = DP_{dextran} \times A_{anomeric,PLAMA}/A_{anomeric,dextran} \quad (3)$$

The GPC trace of dextran-*g*-PLAMA shifted to lower elution time (curve b, Fig. 3), which indicates the increase in molecular weight after the copolymerization. The molecular weight of dextran-*g*-PLAMA determined by GPC was much lower in comparison with that obtained by ^{1}H NMR. The most likely cause of the discrepancy is that the hydrodynamic volume of the linear dextran standard is different from those of dextran-*g*-PLAMA comb-shaped copolymers (Feng et al., 2008; Wang et al., 2011). The actual molecular weights were determined by ^{1}H NMR ($\bar{M}_{n,NMR}$ Table 1).

3.3. Synthesis of dextran-g-(PLAMA-b-PDEGMA) copolymers

One of the unique characteristics of polymers prepared by ATRP is that the dormant alkyl halide chain ends can be reactivated. In this work, the obtained dextran-*g*-PLAMA diblock copolymer was employed as a macroinitiator for the ATRP polymerization of the DEGMA monomer in DMSO at 45 °C, employing the $CuCl/CuCl_2$/bpy catalysts, leading to the preparation of dextran-*g*-(PLAMA-*b*-PDEGMA) triblock copolymers. To study the kinetics of the ATRP polymerizations, aliquots were taken periodically during the ATRP polymerizations and then analyzed with monomer conversion by ^{1}H NMR (Dupayage et al., 2011). After 90 min, monomer conversion reached 73% (targeting DP = 79). The viscosity of the polymerization mixture increased progressively with the conversion, but no microgels or gels formation were detected. As seen in

Table 1
Dextran based biohybrids synthesized by ATRP.

Sample	Reaction time (min)	Conv[c] (%)	$\bar{M}_{n,GPC}$ (g/mol)[d]	$\bar{M}_{n,NMR}$ (g/mol)[e]	Polydispersity index (PDI)[d]	DP_{LAMA}/DP_{DEGMA}[f]	n_{LAMA}/n_{DEGMA}[g]
Dex-$BrMP_{8.3}$[a]	0	0	2.3×10^4		1.74		
Dextran-*g*-$PLAMA_{18}$[a]	30	55.3	7.1×10^4	12.5×10^4	1.67	218/–	18/–
Dextran-*g*-$PLAMA_{23}$[a]	50	66.3	8.9×10^4	15.1×10^4	1.58	273/–	23/–
Dextran-*g*-($PLAMA_{23}$-*b*-$PDEGMA_{30}$)[b]	60	43.1	10.6×10^4	22.0×10^4	1.67	273/365	23/30

[a] Experimental conditions: $[LAMA]_0:[BrMP]_0:[CuCl]_0:[CuCl_2]_0:[bpy]_0 = 40:1:1:0.1:2.5$, initiator = Dex-$BrMP_{8.3}$, [LAMA] = 0.5 M in DMSO at 20 °C.
[b] Experimental conditions: $[DEGMA]_0:[Cl]_0:[CuCl]_0:[CuCl_2]_0:[bpy]_0 = 79:1:1:0.1:2.5$, initiator = dextran-*g*-$PLAMA_{23}$, [DEGMA] = 0.5 M in DMSO at 45 °C.
[c] Overall monomer conversion was determined by ^{1}H NMR spectroscopy.
[d] Estimated by GPC calibrated with linear dextran standards.
[e] $\bar{M}_{n,NMR}$ was calculated by ^{1}H NMR as follows: $\bar{M}_{n,NMR} = \bar{M}_{n,Dex\text{-}BrMP8.3} + DP_{LAMA} \times 469 + DP_{DEGMA} \times 188$.
[f] The composition of the grafted copolymers was calculated according to ^{1}H NMR (Eqs. (3) and (4)).
[g] The average number of LAMA (or DEGMA) units per initiating site (assuming every 12 glucose units possess one initiator site).

Fig. 2 (line d), ATRP polymerizations showed first-order kinetics, indicating a constant concentration of active centers during the polymerizations and termination reactions were not significant. The GPC trace of dextran-*g*-($PLAMA_{23}$-*b*-$PDEGMA_{30}$) showed a very small shift of the peak of the derivatives toward higher molecular weight (curve c, Fig. 3), despite the significant increase in molecular weight (calculated by ^{1}H NMR), which can probably be ascribed to the relatively compact structure maintained by the dextran-*g*-($PLAMA_{23}$-*b*- $PDEGMA_{30}$) copolymers as a consequence of their branched structure (Bontempo et al., 2006). No detectable trace of PDEGMA homopolymers was shown in the GPC traces, confirming the efficient copolymerization.

FT-IR results for the dextran-*g*-($PLAMA_{23}$-*b*-$PDEGMA_{30}$) copolymers were shown in Fig. 1 (curve d). Including the distinct absorbance at 1550 cm^{-1} for the characteristic amide II bonds of PLAMA block, the dextran-*g*-($PLAMA_{23}$-*b*-$PDEGMA_{30}$) presented a broad overlapped OH and NH band at 3390 cm^{-1}, assignable to the residues of the dextran and PLAMA segments. Moreover, two characteristic weak absorbance bands at 840 cm^{-1} and 950 cm^{-1} associated with the repeating oxymethylene units (—OCH_2CH_2—) of PDEGMA indicates the successful synthesis of dextran-*g*-(PLAMA-*b*-PDEGMA) copolymer.

The ^{1}H NMR spectrum of the purified product in DMSO-d_6 (curve c, Fig. S1) revealed the presence of characteristic signals of all these blocks. The DP of the DEGMA block was determined by ^{1}H NMR, based on the integral ratio of resonances at 0.5–1.3 and 5.2 ppm (Eq. (4)):

$$DP_{DEGMA} = DP_{LAMA} \times (A_{0.5\rightarrow1.3} - 3A_{anomeric,LAMA})/3A_{anomeric,LAMA} \quad (4)$$

where $A_{anomeric,LAMA}$ and $A_{0.5\rightarrow1.3}$ are the areas of anomeric protons of PLAMA, and those having chemical shifts between 0.5 and 1.3 ppm (—C***H*****3**,3H protons were assigned to PLAMA and PDEGMA), respectively.

Furthermore, dextran-*g*-($PLAMA_{23}$-*b*-$PDEGMA_{30}$) was analyzed by ^{13}C NMR spectra in D_2O. Compared with the dextran-*g*-$PLAMA_{23}$ macroinitiator, the ^{13}C NMR spectrum of dextran-*g*-($PLAMA_{23}$-*b*-$PDEGMA_{30}$) copolymer clearly showed that, besides the typical signals for the corresponding C-atoms of the dextran-*g*-$PLAMA_{23}$ copolymers, new signals appeared for the PDEGMA grafts, as shown in Fig. S2.

3.4. The thermal properties of the dextran-based biohybrids aqueous solutions

In cases where block copolymers consist of thermo-responsive polymers, the aqueous solution might display a single cloud point at an intermediate temperature. In order to determine the dependence of the thermal properties on temperature, the optical absorbance of the biohybrids solutions was performed by UV–vis spectroscopy (Quan et al., 2009). The optical absorbance of 0.5 wt% aqueous solution of dextran-based biohybrids was monitored at 560 nm at a heating rate of 0.1 °C/min. The LCST was determined as the temperature exhibiting a 50% increase of the total increase in optical absorbance. The results were illustrated in Fig. 4. The diblock glycopolymers of dextran-*g*-$PLAMA_{23}$ were molecularly dissolved in water because of the hydrophilicity of the sugar residues that form hydrogen bonds with the surrounding water molecules. As a consequence, there was no LCST behavior observed for dextran-*g*-$PLAMA_{23}$ up to 53 °C (curve a, Fig. 4). In contract to dextran-*g*-$PLAMA_{23}$, we found the thermally limited solubility of dextran-*g*-($PLAMA_{23}$-*b*-$PDEGMA_{30}$) in water. The aqueous solution of dextran-*g*-($PLAMA_{23}$-*b*-$PDEGMA_{30}$) was transparent at 29 °C, but it suddenly became turbid around 36 °C during the course of heating (curve b, Fig. 4). No precipitate was observed in the turbid solution, when the polymer solution was further heated. The behavior of such phase separation can be ascribed to a subtle hydrophilic–hydrophobic equilibrium for the hydrogen bonding interaction between the PDEGMA segments and water molecules. When the temperature increased above the LCST, hydrogen bonds between ether oxygen atoms of PDEGMA segments and water are broken, and the PDEGMA segments collapse and become hydrophobic (Weber, Hoogenboom, & Schubert, 2012).

Dynamic light scattering (DLS) showed that, at 20 °C, there was one peak, assigned to the unimolecules around 9 nm. At 29 °C, the mean particle size of dextran-g-(PLAMA23-b-PDEGMA30) was about 12 nm. Upon further heating, the polymers existed in solution (at 45 °C) assembled into aggregates with mean size of approximately 60 nm (Fig. S3). Hence, the intermolecular hydrophobic attraction results in the aggregation, which makes it visibly turbid. It is worth noting that the LCST of the copolymers bearing the PDEGMA segments can be adjusted by several molecular parameters, including the different architectures, the chemical nature of

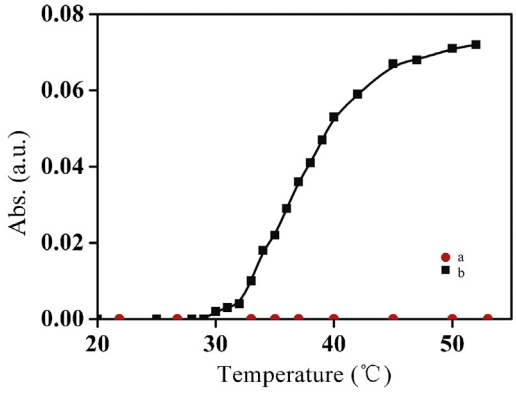

Fig. 4. Plots of turbidity as a function of temperature measured for aqueous solution (5 mg/mL) of (a) dextran-$PLAMA_{23}$ and (b) dextran-*g*-($PLAMA_{23}$-*b*-$PDEGMA_{30}$).

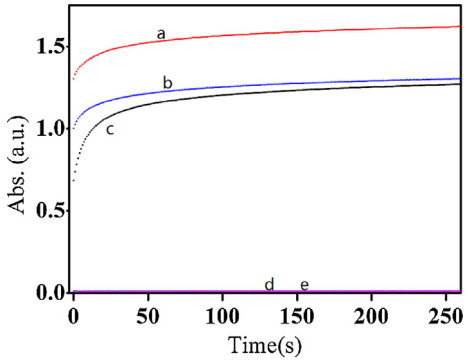

Fig. 5. The interactions of proteins with glycopolymers (a) RCA_{120} (0.5 mg/mL) and dextran-*g*-$PLAMA_{23}$ (0.1 mg/mL), (b) RCA_{120} (0.5 mg/mL) and dextran-*g*-$PLAMA_{18}$ (0.1 mg/mL), (c) RCA_{120} (0.5 mg/mL) and dextran-*g*-($PLAMA_{23}$-*b*-$PDEGMA_{30}$) (0.1 mg/mL), (d) RCA_{120} (0.5 mg/mL) and Dex-$BrMP_{8.3}$ (0.1 mg/mL) and (e) BSA (0.5 mg/mL) and dextran-*g*-$PLAMA_{23}$ (0.1 mg/mL).

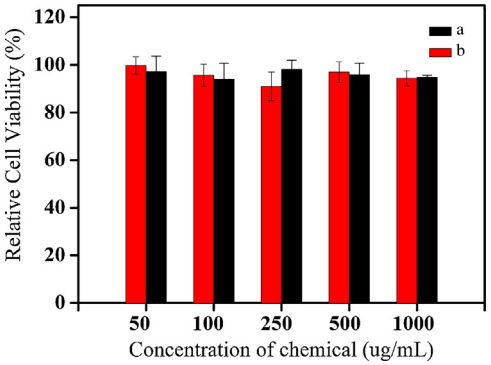

Fig. 6. Cytotoxicity of dextran-based biohybrids in HepG2 cells, (a) dextran-*g*-($PLAMA_{23}$-*b*-$PDEGMA_{30}$) and (b) dextran-*b*-$PLAMA_{23}$. Mean ± standard derivation ($n = 4$).

the polymer backbones and side chain end groups and the length of the PDEGMA blocks (Miasnikova & Laschewsky, 2012; Weber et al., 2012). However, to find the relationships between the LCST values and the structures of dextran-*g*-(PLAMA-*b*-PDEGMA) is beyond our purpose of the present work and will be done in our future work.

3.5. Recognition properties of dextran-derivative glycopolymers

To determine the role of synthetic glycopolymer segments PLAMA for targeting purposes, dextran-*g*-PLAMA and dextran-*g*-(PLAMA-*b*-PDEGMA) based glyco-conjugates were subjected to agglutination assay (RCA_{120}) and BSA was used as a control (Meng, Fang, Wan, Huang, & Xu, 2012). The results are shown in Fig. 5. It was found that the turbidity of dextran-*g*-PLAMA based glycol-conjugates phosphate buffer solution apparently increased after RCA_{120} lectin was added. The result was similar for dextran-*g*-(PLAMA-*b*-PDEGMA). This indicates that the binding between those glyco-conjugates and RCA_{120} lectin occurred and probably resulted in the bigger RCA_{120} cross-linked aggregates, which induced the turbidity change in the solution. This can be further approved by the following DLS assays. When the glycol-conjugates concentration of dextran-*g*-PLAMA and dextran-*g*-(PLAMA-*b*-PDEGMA) were 0.01 mg/mL, glycol-conjugates molecularly dispersed in phosphate buffer solutions (pH7.4) at 20 °C. After RCA_{120} lectin (0.1 mg/mL) was added into the solutions, the big aggregates were generated, as shown in Fig. S4.

Moreover, the turbidity change was not observed for dextran-$BrBP_{8.3}$ in the presence of RCA_{120} (curve d, Fig. 5), due to the lack of galactose specific residues on the dextran chains. Meanwhile, mixing dextran-*g*-PLAMA based glycol-conjugates and BSA did not result in the increase of turbidity (curve e, Fig. 5), which is in agreement with previous literature (Zhou, Dai, & Dong, 2008), showing that PLAMA segments containing galactose groups can specifically bind with RCA_{120} lectin. Aggregates formed in the experiment were then treated with a large excess of free D-galactose (10 mg/mL), a competitive monodentate ligand, and the instant decrease in the absorbance was monitored (Fig. S5). A clear solution was reformed instantly, indicating that the binding of glyco-conjugates and RCA_{120} was replaced by D-galactose. These confirm the specific and reversible interactions of glyco-conjugates to RCA_{120}.

3.6. The in vitro cytotoxicity of dextran-based biohybrids

The biological and biomedical applications of dextran-based biohybrids are highly dependent on their biocompatibility. We therefore, investigated the toxicity of dextran-based biohybrids at different concentrations. In this case, the in vitro cytotoxicity of the dextran-based biohybrids were obtained using the CCK-8 assay on the HepG2 cell line. Here, we use CCK-8 for the determination of cytotoxicity rather than MTT, due to its higher sensitivity for detection (Wu, Xing, Gao, & Chen, 2009). The assay determines the number of viable cells based on the mitochondrial activity of the cells. The highly water-soluble tetrazolium salt [2-(2-methoxy-4-nitrophenyl)-3-(4-nitrophenyl)-5-(2,4-disulfophenyl)-2*H*-tetrazolium monosodium salt] (WST-8) produces a water-soluble formazan dye based on the mitochondrial activity of the cells. Their absorbance can be read at 450 nm, giving the approximate number of viable cells in each well. The wells that contained only the media were used as the negative control, and the wells containing untreated cells were used as the positive control. Each experiment was performed in quadruplicate and cell viability was obtained by dextran-based biohybrids treated cells/absorbance of positive control.

As shown in Fig. 6, dextran were grafted with glycopolymer PLAMA and PLAMA-*b*-PDEGMA individually, and their cytotoxicity values were compared to those of the untreated cells. At very low concentration (50 μg/mL), the cell viability of dextran-*g*-$PLAMA_{23}$ was found to be about 95%. Increasing the concentration of dextran-g-$PLAMA_{23}$ up to 1000 μg/mL did not cause a significant increase in the toxicity of dextran-g-$PLAMA_{23}$, and the cell viability was about 92%. Similarly, at various concentrations (from 50 μg/mL to 1000 μg/mL), the cell viability of dextran-*g*-($PLAMA_{23}$-*b*-$PDEGMA_{30}$) was found to be above 90%. It is apparent from the graph that the cytotoxicity is very low for dextran grafted with PLAMA or PLAMA-*b*-PDEGMA chains. The dextran-based biohybrids may be suitable for use in some potential biomedical applications.

4. Conclusion

A series of dextran-based biodegradable biohybrids containing synthetic glycopolymer chains (PLAMA) and thermo-responsive polymer chains (PDEGMA) have been successfully synthesized via the subsequently ATRP of LAMA and DEGMA monomers using dextran-$BrMP_{8.3}$ as macroinitiator. It is found that the glycopolymer-containing (PLAMA) biohybrids exhibit its specific recongnition for RCA_{120} lectin. In addition, the obtained dextran-*g*-($PLAMA_{23}$-*b*- $PDEGMA_{30}$) possesses the thermosensitive properties with a LCST around 36 °C. Both dextran-*g*-$PLAMA_{23}$ and dextran-*g*-($PLAMA_{23}$-*b*-$PDEGMA_{30}$) showed low cytotoxicity. Thus, the designed dextran-derivative biohybrids have high potential for biomedical applications such as targeted drug delivery systems.

Acknowledgements

This work is supported by the National Natural Science Foundation of China (Grant Nos. 51028301 and 21174146) Programs and subsidized by the Special Funds for National Basic Research Program of China (Grant No. 2009CB930100).

Appendix A. Supplementary data

Supplementary data associated with this article can be found, in the online version, at http://dx.doi.org/10.1016/j.carbpol.2013.09.020.

References

Bajgai, M. P., Parajuli, D. C., Ko, J. A., Kang, H. K., Khil, M. S., & Kim, H. Y. (2009). Synthesis, characterization and aqueous dispersion of dextran-g-poly(1,4-dioxan-2-one) copolymers. *Carbohydrate Polymers*, *78*(4), 833–840.

Becer, C. R. (2012). The glycopolymer code: Synthesis of glycopolymers and multivalent carbohydrate–lectin interactions. *Macromolecular Rapid Communications*, *33*(9), 742–752.

Bontempo, D., Masci, G., De Leonardis, P., Mannina, L., Capitani, D., & Crescenzi, V. (2006). Versatile grafting of polysaccharides in homogeneous mild conditions by using atom transfer radical polymerization. *Biomacromolecules*, *7*(7), 2154–2161.

Dai, X. H., Dong, C. M., & Yan, D. Y. (2008). Supramolecular and biomimetic polypseudorotaxane/glycopolymer biohybrids: Synthesis, glucose-surfaced nanoparticles, and recognition with lectin. *Journal of Physical Chemistry B*, *112*(12), 3644–3652.

Dupayage, L., Nouvel, C., & Six, J. L. (2011). Protected versus unprotected dextran macroinitiators for ATRP synthesis of Dex-g-PMMA. *Journal of Polymer Science Part a-Polymer Chemistry*, *49*(1), 35–46.

Dupayage, L., Nouvel, C., & Six, J. L. (2012). Copper-mediated ATRP of MMA in DMSO from unprotected dextran macroinitiators. *Polymer Bulletin*, *68*(3), 647–665.

Dupayage, L., Save, M., Dellacherie, E., Nouvel, C., & Six, J. L. (2008). PMMA-grafted dextran glycopolymers by atom transfer radical polymerization. *Journal of Polymer Science Part a-Polymer Chemistry*, *46*(23), 7606–7620.

Feng, C., Shen, Z., Gu, L. N., Zhang, S., Li, L. T., Lu, G. L., et al. (2008). Synthesis and characterization of PNIPAM-b-(PEA-g-PDEA) double hydrophilic graft copolymer. *Journal of Polymer Science Part a-Polymer Chemistry*, *46*(16), 5638–5651.

Feng, W. Q., Lv, W. P., Qi, J. J., Zhang, G. L., Zhang, F. B., & Fan, X. B. (2012). Quadruple-responsive nanocomposite based on dextran–PMAA–PNIPAM, iron oxide nanoparticles, and gold nanorods. *Macromolecular Rapid Communications*, *33*(2), 133–139.

Heinze, T., Liebert, T., Heublein, B., & Hornig, S. (2006). Functional polymers based on dextran. *Polysaccharides II*, *205*, 199–291.

Hu, Z. G., Fan, X. S., & Zhang, G. S. (2010). Synthesis and characterization of glucose-grafted biodegradable amphiphilic glycopolymers P(AGE-glucose)-b-PLA. *Carbohydrate Polymers*, *79*(1), 119–124.

Lemechko, P., Renard, E., Guezennec, J., Simon-Colin, C., & Langlois, V. (2012). Synthesis of dextran-graft-PHBHV amphiphilic copolymer using click chemistry approach. *Reactive & Functional Polymers*, *72*(8), 487–494.

Lutz, J. F. (2011). Thermo-switchable materials prepared using the OEGMA-platform. *Advanced Materials*, *23*(19), 2237–2243.

Lv, W. P., Liu, S. Q., Feng, W. Q., Qi, J. J., Zhang, G. L., Zhang, F. B., et al. (2011). Temperature- and redox-directed multiple self assembly of poly(N-isopropylacrylamide) grafted dextran nanogels. *Macromolecular Rapid Communications*, *32*(14), 1101–1107.

Matyjaszewski, K., Shipp, D. A., Wang, J. L., Grimaud, T., & Patten, T. E. (1998). Utilizing halide exchange to improve control of atom transfer radical polymerization. *Macromolecules*, *31*(20), 6836–6840.

Meng, X. L., Fang, Y., Wan, L. S., Huang, X. J., & Xu, Z. K. (2012). Glycopolymer brushes for the affinity adsorption of RCA(120): Effects of thickness, grafting density, and epitope density. *Langmuir*, *28*(38), 13616–13623.

Miasnikova, A., & Laschewsky, A. (2012). Influencing the phase transition temperature of poly(methoxy diethylene glycol acrylate) by molar mass, end groups, and polymer architecture. *Journal of Polymer Science Part a-Polymer Chemistry*, *50*(16), 3313–3323.

Miura, Y. (2012). Design and synthesis of well-defined glycopolymers for the control of biological functionalities. *Polymer Journal*, *44*(7), 679–689.

Monge, S., Darcos, V., & Haddleton, D. M. (2004). Effect of DMSO used as solvent in copper mediated living radical polymerization. *Journal of Polymer Science Part a-Polymer Chemistry*, *42*(24), 6299–6308.

Munoz-Bonilla, A., Heuts, J. P. A., & Fernandez-Garcia, M. (2011). Glycoparticles and bioactive films prepared by emulsion polymerization using a well-defined block glycopolymer stabilizer. *Soft Matter*, *7*(6), 2493–2499.

Nagatsuka, T., Uzawa, H., Sato, K., Ohsawa, I., Seto, Y., & Nishida, Y. (2012). Glycotechnology for decontamination of biological agents: A model study using ricin and biotin-tagged synthetic glycopolymers. *Acs Applied Materials & Interfaces*, *4*(2), 832–837.

Narain, R., & Armes, S. P. (2003). Synthesis and aqueous solution properties of novel sugar methacrylate-based homopolymers and block copolymers. *Biomacromolecules*, *4*(6), 1746–1758.

Narumi, A., & Kakuchi, T. (2008). Synthesis of glycoconjugated branched macromolecular architectures. *Polymer Journal*, *40*(5), 383–397.

Otsuka, I., Travelet, C., Halila, S., Fort, S., Pignot-Paintrand, I., Narumi, A., et al. (2012). Thermoresponsive self-assemblies of cyclic and branched oligosaccharide-block-poly(N-isopropylacrylamide) diblock copolymers into nanoparticles. *Biomacromolecules*, *13*(5), 1458–1465.

Patrizi, M. L., Piantanida, G., Coluzza, C., & Masci, G. (2009). ATRP synthesis and association properties of temperature responsive dextran copolymers grafted with poly(N-isopropylacrylamide). *European Polymer Journal*, *45*(10), 2779–2787.

Pfaff, A., Schallon, A., Ruhland, T. M., Majewski, A. P., Schmalz, H., Freitag, R., et al. (2011). Magnetic and fluorescent glycopolymer hybrid nanoparticles for intranuclear optical imaging. *Biomacromolecules*, *12*(10), 3805–3811.

Polikarpov, N., Appelhans, D., Welzel, P., Kaufmann, A., Dhanapal, P., Bellmann, C., et al. (2012). Tailoring uptake and release of ATP by dendritic glycopolymer/PNIPAAm hydrogel hybrids: First approaches towards multicompartment release systems. *New Journal of Chemistry*, *36*(2), 438–451.

Quan, C. Y., Wu, D. Q., Chang, C., Zhang, G. B., Cheng, S. X., Zhang, X. Z., et al. (2009). Synthesis of thermo-sensitive micellar aggregates self-assembled from biotinylated PNAS-b-PNIPAAm-b-PCL triblock copolymers for tumor targeting. *Journal of Physical Chemistry C*, *113*(26), 11262–11267.

Siegwart, D. J., Oh, J. K., & Matyjaszewski, K. (2012). ATRP in the design of functional materials for biomedical applications. *Progress in Polymer Science*, *37*(1), 18–37.

Sun, G. M., & Mao, J. J. (2012). Engineering dextran-based scaffolds for drug delivery and tissue repair. *Nanomedicine*, *7*(11), 1771–1784.

Voit, B., & Appelhans, D. (2010). Glycopolymers of various architectures-more than mimicking nature. *Macromolecular Chemistry and Physics*, *211*(7), 727–735.

Wang, Y. X., Zhang, X. G., Han, Y. C., Cheng, C., & Li, C. X. (2012). pH- and glucose-sensitive glycopolymer nanoparticles based on phenylboronic acid for triggered release of insulin. *Carbohydrate Polymers*, *89*(1), 124–131.

Wang, Z. H., Li, W. B., Ma, J., Tang, G. P., Yang, W. T., & Xu, F. J. (2011). Functionalized nonionic dextran backbones by atom transfer radical polymerization for efficient gene delivery. *Macromolecules*, *44*(2), 230–239.

Wang, Z. H., Zhu, Y., Chai, M. Y., Yang, W. T., & Xu, F. J. (2012). Biocleavable comb-shaped gene carriers from dextran backbones with bioreducible ATRP initiation sites. *Biomaterials*, *33*(6), 1873–1883.

Weber, C., Hoogenboom, R., & Schubert, U. S. (2012). Temperature responsive biocompatible polymers based on poly(ethylene oxide) and poly(2-oxazoline)s. *Progress in Polymer Science*, *37*(5), 686–714.

Wu, S. N., Xing, D., Gao, X. J., & Chen, W. R. (2009). High fluence low-power laser irradiation induces mitochondrial permeability transition mediated by reactive oxygen species. *Journal of Cellular Physiology*, *218*(3), 603–611.

Xu, N., Wang, R., Du, F. S., & Li, Z. C. (2009). Synthesis of amphiphilic biodegradable glycocopolymers based on poly(epsilon-caprolactone) by ring-opening polymerization and click chemistry. *Journal of Polymer Science Part a-Polymer Chemistry*, *47*(14), 3583–3594.

Zhou, W., Dai, X. H., & Dong, C. M. (2008). Biodegradable and biomimetic poly(epsilon-caprolactone)/poly(lactobionarnidoethyl methacrylate) biohybrids: Synthesis, lactose-installed nanoparticles and recognition properties. *Macromolecular Bioscience*, *8*(3), 268–278.